

Clinical or ATPase domain mutations in ABCD4 disrupt the interaction between the vitamin B₁₂-trafficking proteins ABCD4 and LMBD1

Victoria Fettelschoss^a, Patricie Burda^a, Corinne Sagné^b, David Coelho^c, Corinne De Laet^d, Seraina Lutz^a, Terttu Suormala^a, Brian Fowler^a, Nicolas Pietrancosta^e, Bruno Gasnier^b, Beat Bornhauser^f, D. Sean Froese^{a,g,1}, Matthias R. Baumgartner^{a,g,h,1}

^aDivision of Metabolism and Children's Research Center, University Children's Hospital, CH-8032 Zurich, Switzerland

^bNeurophotonics Laboratory UMR 8250, Paris Descartes University, Centre National de la Recherche Scientifique, Sorbonne Paris Cité, F-75006 Paris, France

^cUMR_S UL-Inserm U954 Nutrition-Genetics-Environmental Risk Exposure and Reference Centre of Inborn Metabolism Diseases, Medical Faculty of Nancy University and University Hospital Centre, Nancy, France

^dNutrition and Metabolism Unit, University Children's Hospital Queen Fabiola, Free University of Brussels (ULB), 1020, Brussels, Belgium.

^eCBMIT team, UMR 8601, Paris Descartes University, Centre National de la Recherche Scientifique, Sorbonne Paris Cité, F-75006 Paris, France

^fDepartment of Oncology, Children's Research Center, University Children's Hospital, Zurich, Switzerland

^gradiz – Rare Disease Initiative Zurich, Clinical Research Priority Program for Rare Diseases, University of Zurich, Switzerland

^hZurich Center for Integrative Human Physiology, University of Zurich, Switzerland

Running title: ABCD4 and LMBD1 interaction disruption

¹Equal contribution and to whom correspondence may be addressed:

Prof. Matthias R. Baumgartner, Division of Metabolism and Children's Research Center, University Children's Hospital, Steinweisstrasse 75, CH-8032 Zurich, Switzerland, Telephone: +41 (0)44 266 7722; Fax: +41 (0)44 266 7167; Email: matthias.baumgartner@kispi.uzh.ch and Dr. D. Sean Froese, Division of Metabolism and Children's Research Center, University Children's Hospital, Steinweisstrasse 75, CH-8032 Zurich, Switzerland, Telephone: +41 (0)44 266 7156; Fax: +41 (0)44 266 7167; Email: sean.froese@kispi.uzh.ch

Keywords: protein-protein interaction, fluorescence resonance energy transfer (FRET), lysosome, inborn error of metabolism, ABC ATPase, ATP-binding cassette transporter family, LMBD1, vitamin B12, cblJ, cblF, ABCD4

ABSTRACT

Vitamin B₁₂ (cobalamin, Cbl), in the cofactor forms methyl-Cbl and adenosyl-Cbl, is required for the function of the essential enzymes methionine synthase and methylmalonyl-CoA mutase, respectively. Cbl enters mammalian cells by receptor-mediated endocytosis of protein-bound Cbl followed by lysosomal export of free Cbl to the cytosol, and further processing to these cofactor forms. The integral membrane proteins LMBD1 and ABCD4 are required for lysosomal release of Cbl, and mutations in the genes *LMBRD1* and *ABCD4* result in the cobalamin metabolism disorders cblF and cblJ. We report a new (fifth) patient with the cblJ disorder, who presented at 7 days of age with poor feeding, hypotonia, methylmalonic aciduria, and elevated plasma homocysteine and harbored the mutations c.1667_1668delAG [p.Glu556Glyfs*27] and c.1295G>A [p.Arg432Gln] in the *ABCD4* gene. Cbl cofactor forms are decreased in fibroblasts from this patient, but could be rescued by over-expression of either ABCD4 or, unexpectedly, LMBD1. Utilizing a sensitive live-cell FRET assay, we demonstrated selective interaction between ABCD4 and LMBD1, and decreased interaction when ABCD4 harbored the patient mutations p.Arg432Gln or p.Asn141Lys, or artificial mutations disrupting the ATPase domain. Finally, we showed that ABCD4 lysosomal targeting depends on co-expression of, and interaction with, LMBD1. These data broaden the patient and mutation spectrum of cblJ deficiency, establish a sensitive live-cell assay to detect the LMBD1-ABCD4 interaction, and confirm the importance of this interaction for proper intracellular targeting of ABCD4 and cobalamin cofactor synthesis.

INTRODUCTION

Vitamin B₁₂ (cobalamin, Cbl) is required for the function of two enzymes, cytosolic methionine synthase (MS) and mitochondrial methylmalonyl-CoA mutase (MUT), and a sophisticated pathway of cellular transport and modification is required for production and targeting of their appropriate cofactor forms. This elaborate pathway is likely an evolutionary response to the scarcity and reactivity of Cbl (1,2), and presents Cbl with a cellular odyssey to reach these targets. Cbl's intracellular journey begins with receptor mediated endocytosis following binding of Cbl-bound transcobalamin to the transcobalamin receptor (3). Once internalized, Cbl is released from

transcobalamin as the pH lowers in the transition from the endosome to lysosome. Free Cbl is transported out of the lysosome and into the cytosol, a process that requires two integral membrane proteins, LMBD1 and ABCD4 (4,5). Within the cytosol, Cbl is bound and processed by the protein MMACHC (6,7), and, via interaction with MMACHC, targeted by MMADHC (8,9) either (i) to cytosolic MS, with subsequent conversion to methyl-Cbl (MeCbl) requiring MS reductase (encoded by *MTRR*), or (ii) to the mitochondria, for uptake by an unknown mechanism. Within the mitochondria, Cbl is adenosylated by MMAB to form the functional cofactor adenosyl-Cbl (AdoCbl), and then transferred to MUT (10), an action closely controlled by MMAA, which blocks or ejects non-functional Cbl forms (11). The molecular actions of these post lysosomal pathway proteins are now quite well elucidated, enabled by their solubility and accessibility to recombinant production; however, those of the membrane bound proteins, *viz.* LMBD1 and ABCD4, remain elusive.

Approximately 30 years ago Rosenblatt *et al.* (12) published the finding of a B₁₂ defective patient whose fibroblasts were unable to release Cbl from the lysosome. This disorder, termed cblF (methylmalonic aciduria and homocystinuria, cblF type; OMIM: #277380; (13)), was eventually found to be due to defective LMBD1 (*LMBRD1* gene) (5), an integral membrane protein with homology to the lipocalin-1 interacting membrane receptor LIMR. LMBD1 colocalizes with LAMP1 (5), a lysosomal membrane protein, providing a direct link between the mutated protein and the organelle of the defect. However, the way in which LMBD1 facilitates lysosomal Cbl release is not yet clear. By homology to LIMR, which binds and internalizes lipocalins, small secreted proteins which bind protoporphin IX among other ligands (14), a receptor/transporter role has been suggested (5). Further, and of as yet unknown significance, a recent study suggested a small percentage (~3.4%) of LMBD1 is retained at the plasma membrane, and is important for insulin receptor internalization (15). Thus far all 16 patients with recessive mutations in *LMBRD1* have presented with the cblF type disorder (5,16-19) without apparent glucose metabolism dysregulation.

More recently, a second protein involved in lysosomal Cbl release was discovered. Deficiency of ABCD4, an ABC-transporter family protein, stemming from truncating or missense mutations in

the *ABCD4* gene, results in methylmalonic aciduria and homocystinuria, cblJ type (OMIM: #614857) (4). Although in patient fibroblasts cblJ deficiency phenotypically mimics cblF, including loss of Cbl transport out of the lysosome, somatic complementation assays and the inability of over-expressed LMBD1 to rescue cobalamin cofactor synthesis in cblJ cells firmly establish them as separate disorders. Only four patients have been described in detail thus far with cblJ deficiency. The first two described patients presented within the first weeks of life with feeding difficulties, hypotonia, respiratory distress (patient 1) and an atrial septal defect (patient 2), among many further symptoms (4). Both patients were heterozygous for a splicing or truncating mutation and a missense mutation, which in the case of patient 2, was also found to affect splicing (4). By contrast, patients three (20) and four (21) both harboured the same homozygous missense mutation (c.423C>G, p.Asn141Lys), presented between 8 and 12 years of age and had less severe symptoms, including mild macrocytic anaemia and hyperpigmentation. Presentation with hyperpigmentation is unusual for patients with inborn errors of cobalamin metabolism, although there are rare reports of hyperpigmentation in general vitamin B₁₂ deficiency (e.g. (22-24)). Hyperpigmentation has not been noted in any of the 16 patients with LMBD1 deficiency (5,16-19), although some patients had skin rash or eczema.

While other ABCD family members (1-3) are peroxisomal (25-28), ABCD4 lacks the N-terminal peroxisomal targeting hydrophobic motif (29). Over-expressed ABCD4 has been identified in the ER (30), however, over-expression in the presence of LMBD1 resulted in lysosomal targeting (31). Lysosomal targeting is in line with previous identification of colocalization between ABCD4, LMBD1 and LAMP1, a classical lysosomal marker (4), its identification in a large scale proteomics study of lysosomal membrane proteins (32), and the cellular inability to release Cbl from the lysosomes in the case of either the cblF or cblJ defect. LMBD1-dependent targeting of ABCD4, along with the cellular and biochemical mimicry of ABCD4 and LMBD1 dysfunction suggests they interact, a possibility partially supported by surface plasmon resonance of purified proteins *in vitro* (33).

Here, we report a new patient, the fifth with cblJ deficiency who presented with mild disease due to a truncating and a missense mutation in the *ABCD4* gene. The unusual ability of over-expressed

LMBD1 to correct the cellular phenotype in fibroblasts in this patient prompted us to further investigate the cellular location and interaction of these partner proteins. Using a live cell FRET-assay, we provide experimental evidence of the LMBD1-ABCD4 interaction in human fibroblasts and highlight the crucial importance of this interaction and its disturbance by patient mutations or mutations which disrupt ATPase activity of ABCD4. We further confirm the lysosomal localization of LMBD1 and targeting of ABCD4 to the lysosome in the presence of LMBD1, which is prevented when the ability of ABCD4 to bind LMBD1 is broken. These data suggest an intimate relationship between ABCD4 and LMBD1, and describe how ABCD4 mutations affect the interaction with LMBD1, impair lysosomal targeting and ultimately ABCD4 function.

RESULTS

A new patient with cblJ deficiency – The first child of non-consanguineous parents was born at full-term after an uneventful pregnancy. Neonatal screening suggested methylmalonic aciduria, with increased propionyl-carnitine. At 7 days of age he presented with hypotonia and poor feeding. Methylmalonic acid in the urine was 403 mmol/mol creatinine and plasma total homocysteine was 88.6 µmol/L. These clinical and biochemical findings would be consistent with vitamin B₁₂ deficiency or disturbed B₁₂ metabolism, although the clinical symptoms are unspecific at this age. From the first week of life the patient received 1 mg of vitamin B₁₂ every 2 days and a protein-restricted diet. Eight days after the start of therapy methylmalonic acid levels decreased to 77 mmol/mol creatinine (ref < 3). Follow-up neurological examination was normal.

The patient was lost to follow-up between the ages of 2 and 10 years. During this period, vitamin B₁₂ (1 mg/d) *p.o.* was regularly taken. His visit at the age of 10 years was motivated by a deterioration of vision (6/10 and 1/10). Eye investigations showed a retinal dystrophy and a loss of the scotopic reaction at the electroretinogram. Neurophysiologic evaluation (electromyography, conduction velocity, evoked potential) suggested a peripheral neuropathy and a slight involvement of the pyramidal tract. Retinopathy as well as peripheral neuropathy and involvement of the spinal tract are common in early onset cblC deficiency and other defects of methylcobalamin synthesis (such as cblD, cblE, or cblG), while in nutritional vitamin

B₁₂ deficiency retinopathy is rarely found. Brain and spine MRI were normal. He also presented with regular pain and weakness of the lower limbs as well as hypopigmentation of the hair. Increased total homocysteine, urinary methylmalonate, macrocytosis and albuminuria were present at that time (Table 2). Treatment was intensified: folic acid was added and hydroxocobalamin was given *i.m.* daily during the first week, then 3 times per week and finally once a week. The biochemical tests improved progressively and normalized after 4 months.

Cobalamin uptake and coenzyme synthesis (CCS) assay of cultured primary fibroblasts of the patient showed elevated uptake of radioactive cyanocobalamin compared to controls, but severely decreased production of the cofactor forms AdoCbl and MeCbl (Suppl Table S2), suggesting either cblF or cblJ deficiency. Molecular genetic investigation revealed no mutations in *LMBRD1*, the gene responsible for the cblF defect, whereas a 2 base-pair deletion resulting in a frame-shift (c.1667_1668delAG, p.Glu556Glyfs*27) was found in trans with a 1 base-pair substitution resulting in a missense mutation (c.1295G>A p.Arg432Gln) in *ABCD4*, the gene responsible for the cblJ complementation group. The missense mutation is predicted to be “deleterious” by SWIFT and “probably damaging” by PolyPhen and has been identified in only 1 out of 121,412 alleles in the EXAC database (www.exac.broadinstitute.org). Therefore, this patient has been assigned as the fifth patient with the cblJ defect (cblJ05). As found with another reported patient with the cblJ defect (20), incorporation of [¹⁴C]propionate and formation of [¹⁴C]methionine from [¹⁴C]formate were within reference ranges (data not shown), and therefore too high to allow somatic complementation analysis.

Unusual correction of intracellular cblJ deficiency with LMBD1 over-expression – To further evaluate intracellular deficiency in cblF and cblJ patient fibroblasts, we attempted cellular cobalamin cofactor synthesis rescue using over-expression of wild-type (wt) untagged versions of either LMBD1 or ABCD4 using the pTracer-CMV2 vector (Figure 1A). Immortalized fibroblasts from cblJ01 and cblJ02 have rescued production of AdoCbl and MeCbl in the presence of over-expression of ABCD4 but not LMBD1. A representative immortalized cblF cell line was partially rescued by ABCD4, but has much greater production of both AdoCbl and MeCbl following

LMBD1 over-expression, consistent with previous results (4). By contrast, synthesis of both cofactor forms was equally rescued by over-expression of either ABCD4 or LMBD1 in immortalized cblJ05 fibroblasts.

The combination of cofactor synthesis rescue by either LMBD1 or ABCD4 over-expression in the cblJ05 fibroblasts with the almost identical clinical and biochemical presentation of cblF and cblJ patients (4), led us to suggest that ABCD4 and LMBD1 may operate in concert to perform their biochemical functions. In order to test this hypothesis, we generated plasmids consisting of LMBD1 tagged C-terminally with enhanced green fluorescent protein (GFP) and ABCD4 tagged C-terminally with far-red fluorescent protein (fRFP). To ensure that these fusion constructs (LMBD1-GFP and ABCD4-fRFP) represented physiologically functional proteins, we repeated the CCS assay following transfection of cblF and cblJ02 with both constructs (Figure 1B). cblJ02 was chosen here because all other cblJ fibroblast cell lines carry at least one missense mutation in ABCD4 (Table 1), potentially resulting in residual endogenous mutant ABCD4 protein which may affect our experiments. Control fibroblasts are able to generate approximately 20% AdoCbl (\pm 5%, range: 12-28%) and 38% MeCbl (\pm 11%, range: 22-55%) as total cellular cobalamin from [⁵⁷Co]cyanocobalamin. When transfected with constructs coding for GFP only (cblF) or fRFP only (cblJ), patient fibroblasts produced almost negligible amounts of both cofactors. However, production of each cofactor was elevated following expression of the fluorescently-tagged proteins (LMBD1-GFP and ABCD4-fRFP) to similar levels as over-expressed with untagged protein (LMBD1 or ABCD4) from pTracer-CMV2. Therefore, although there are currently no direct assays of either LMBD1 or ABCD4 function, the fluorescently-tagged LMBD1 and ABCD4 proteins are functional as assessed by their ability to rescue AdoCbl and MeCbl synthesis in the respective deficient cell lines.

Intracellular targeting of ABCD4 and LMBD1 – As a first test to identify whether LMBD1 and ABCD4 are required for mutual function, we examined their subcellular location using confocal microscopy. Following co-transfection of LMBD1-GFP and ABCD4-fRFP into control fibroblasts, both proteins were found to co-localize with each other as well as with endogenous lysosomal

LAMP1 (Figure 2A). However, when expressed separately, LMBD1 extensively colocalized with LAMP1 (Figure 2B), while ABCD4 and LAMP1 showed very little colocalization and only at the cell periphery (Figure 2C). These results were confirmed by comparison of each protein with LysoTracker, whereby LMBD1 and LAMP1, but not ABCD4, showed extensive lysosomal localization (Suppl Figure S1). Following site-directed mutagenesis to incorporate the mistargeting mutation p.Tyr232Ala into LMBD1-GFP, shown previously to inhibit LMBD1 internalization from the plasma membrane to the lysosome (15), ABCD4-fRFP was found to follow LMBD1 to its altered cellular location in both HeLa cells and control fibroblasts (Suppl Figure S2). This confirms that ABCD4 targeting is at least partially mediated by LMBD1, and suggests that in the absence of over-expressed LMBD1, the low levels of endogenous LMBD1 present in these cells are unable to efficiently direct ABCD4 to the lysosome. Although over-expressed ABCD4 alone has been previously described to be found sequestered in the endoplasmic reticulum (30,31), we did not find significant overlap of individually over-expressed ABCD4-fRFP with a marker of the ER in control fibroblasts (Suppl Figure S3) or HeLa cells (data not shown). Of the organelles surveyed, including early- (EEA), late- (Rab7), and recycling (Rab11) endosomes, as well as ER (HSP47), peroxisomes (ABCD3) and autophagosomes (LC3), ABCD4-fRFP overlapped best with autophagosomes (Suppl Figure S3). Of note, this overlap was found mostly in the perinuclear region (Suppl Figure S3), the region in which there was poor colocalization between ABCD4-fRFP and LAMP1 (Figure 2C). Finally, although co-expression of ABCD4 and LMBD1 was required for significant lysosomal targeting of ABCD4 (Figure 2), it did not lead to increased cofactor synthesis in *cb1J* deficient fibroblasts compared to over-expression of ABCD4 alone (Figure 1B).

Specific detection of the LMBD1-GFP and ABCD4-fRFP interaction by FACS based FRET – Given the importance of LMBD1 for lysosomal targeting of ABCD4, we utilized a sensitive live cell assay to detect protein-protein interaction based on fluorescent resonance energy transfer (FRET) of the fluorescently-labelled proteins using a fluorescence activated cell sorter (FACS). Since FACS based FRET, to our knowledge, has been until now only been performed using the CFP::YFP conjugate pair

(e.g. (34-38)) we tested the amenability of this method to our GFP and fRFP pair as FRET donor and acceptor, respectively. In immortalized control fibroblasts gated according to forward and side scatter (FSC/SSC) to identify only living cells (Suppl Figure S4), the FRET positive signal (FRET+) could be clearly distinguished in cells transfected with a fusion construct of GFP tethered to fRFP (GFP::fRFP) from signal found in untransfected fibroblasts (negative), those expressing GFP or fRFP only, or those co-transfected with GFP and fRFP (Suppl Figure S4). Thus, with appropriate gating, 75.5% of live cells transfected with the fusion construct were found to be FRET+, compared to 0.1% when cells were co-transfected with GFP and fRFP (Suppl Figure S4). This clearly demonstrates the feasibility of using a flow cytometer to detect FRET+ signal from the chosen fluorescent proteins.

As with the GFP::fRFP fusion protein, we constructed a fusion protein of LMBD1-GFP::ABCD4-fRFP (Suppl Figure S5) to function as a positive control in our further FRET assays. Following transfection of this construct into fibroblasts, 48% of cells had elevated signal in the GFP channel (GFP+, Figure 3A, %GFP), and 47% of cells had elevated signal in the far-red channel (fRFP+, Figure 3A, %fRFP). From the GFP+ and fRFP+ cells, the mean intensity (MI) of the FRET signal, a measure of FRET independent of our final gating (see below), was 140 (Figure 3A, FRET intensity). This fusion protein gave a linear GFP vs FRET signal (Figure 3B), which we gated as FRET+, and encompassed 24% of all cells, and 59% of cells which were both GFP+ and fRFP+ (Figure 3C). When co-transfected, LMBD1-GFP and ABCD4-fRFP showed similar transfection efficiencies (37% GFP+ and 46% fRFP+ cells) to those of the fusion protein, and an MI of 114 (Figure 3A). The GFP vs FRET signal pattern was also similar, with 17% of all cells (Figure 3B) and 50% of the GFP+ and fRFP+ cells (Figure 3C) falling within the FRET+ gate. LMBD1-GFP and ABCD4-fRFP transfected separately, although well expressed, resulted in no (<0.5%) FRET+ signal (Suppl Figure S6). To establish the specificity of this assay, we analysed FRET signal against two lysosomal membrane proteins, LAMP1 and ABCB9, which are not involved in *Cbl* transport. Each protein conjugated to fRFP was co-transfected with LMBD1-GFP, or conjugated to GFP co-transfected with ABCD4-fRFP. These alternate

lysosomal membrane proteins, although well expressed (Figure 3A), gave FRET+ signals in all cells ranging from 0 – 4% (Figure 3B), and in GFP+ and fRFP+ cells ranging from 1 – 8% (Figure 3C), with FRET MIs of 23 – 43 (Figure 3A), all clearly below co-transfected LMBD1 and ABCD4. The complete FACS data is summarized in the Table in Figure 3D, and allow us to conclude that LMBD1-GFP and ABCD4-fRFP have a specifically increased FRET signal, indicative of protein-protein interaction.

ABCD4 patient and ATPase disrupting mutations reduce interaction and function – Based on the ability to sensitively detect interaction between ABCD4 and LMBD1, we investigated whether the missense mutation found in our patient (p.Arg432Gln) affected this interaction (Figure 4). We further chose to reproduce the effects of the missense mutation p.Asn141Lys (p.N141K), which has been found homozygously in two patients with the *cbfJ*-type defect (20,21). Additionally, we generated two mutations in the ATPase domain: p.Asp548Asn (p.D548N) in the Walker B motif, which was previously shown to inhibit function (4), and a double mutation, p.Gly426_Lys427delinsAlaLeu (p.G426A/K427L) in the Walker A motif, to test whether disruption of ATPase activity in this protein affected interaction with LMBD1. For a schematic of the position of these mutations in ABCD4 see Figure 5A. Since no disease causing missense mutations has been found thus far in LMBD1, and it is as yet unclear which domains might be required for LMBD1 function, we did not produce any mutations in this protein.

Following co-transfection with LMBD1-GFP, all four mutant proteins resulted in markedly decreased FRET+ signal compared to wt ABCD4-fRFP (Figure 4A), of which the ATPase double mutation p.Gly426_Lys427delinsAlaLeu resulted in essentially no FRET+ signal (Figure 4A). This despite good expression of all mutant constructs (Suppl Figure S7) and only slightly decreased FRET+ signal for the single mutations p.Gly426Ala and p.Lys427Leu (Suppl Figure S8). To investigate whether this decreased interaction with LMBD1 resulted in altered cellular localization of ABCD4, we performed confocal microscopy. Wild-type ABCD4-fRFP showed strongly overlapping signal with LMBD1-GFP, which was quantified using the Pearson correlation co-efficient (PCC = 0.93). The ABCD4 proteins harbouring the two patient mutations were also predominantly found in the

same cellular location as LMBD1 (PCC = 0.83-0.86, Figure 4B). ABCD4 proteins with the ATPase mutation p.Asp548Asn appeared to be inside as well as on the membrane of the lysosome (Figure 4B), suggesting in addition to proper lysosomal localization, they may be internalized, perhaps for degradation. Consistent with a complete loss of FRET+ signal, ABCD4-fRFP with the p.Gly426_Lys427delinsAlaLeu mutation only partially overlapped with LMBD1 (PCC = 0.54, Figure 4C). The results of both of these techniques are consistent with results of the CCS assay of ABCD4 protein function, whereby ABCD4 harbouring the mutations p.Asn141Lys and p.Arg432Gln were less able to rescue cofactor synthesis in *cbfJ* fibroblasts than wt protein, p.Asp548Asn had even decreased rescue and p.Gly426_Lys427delinsAlaLeu resulted in essentially no rescue at all.

Homology modeling of the ATPase domain of ABCD4 accounts for the effect of patient fifth mutations – To assess how the p.Arg432Gln mutation might alter the interaction between ABCD4 and LMBD1, we built an atomic-resolution model of the ATPase domain of human ABCD4 using homology modeling of the crystal structure of the multiple sugar binding transport ATP-binding protein from *Pyrococcus horikoshii* (Protein Data Bank ID #2D62) as a template and refined using PCAT1 from *Ruminiclostridium thermocellum* (ID #4RY2) (Figure 5B). Interestingly, the resulting 3D model predicts that Arg432 is on a solvent accessible surface and its side chain extends outwardly and away from the modeled nucleotide, in agreement with a potential role in physical interaction with another protein but not in nucleotide hydrolysis. By contrast, Lys427 and Asp548 extend towards the phosphate groups of the bound nucleotide, consistent with their roles in the Walker A and B motifs, respectively (Suppl Figure S9B). Finally, the frameshift mutation p.Glu556Glyfs*27 carried by the second allele of patient fifth should delete two alpha helices and three beta strands (Suppl Figure S9), thus disrupting the ATPase domain structure and resulting in a null allele of ABCD4.

DISCUSSION

A fifth patient with the cbfJ intracellular metabolism of cobalamin disorder – Here we

present the fifth patient in the literature with the cblJ defect, although besides the other four published patients at least one other patient is known (Jesina et al., abstract P-586 in (39)). Our patient presented within the first week of life with hypotonia and poor feeding, more reminiscent of patients 1 and 2. He also responded well to therapy including vitamin B₁₂, similar to patients 1, 3 and 4. Patient 2's response was complicated by many other factors, including delayed diagnosis, but also showed a partial clinical and metabolic response to cobalamin supplementation (4). As with related disorders, this reinforces the importance of swift diagnosis and treatment.

Our patient also had hair hypopigmentation. cblJ patient 3 was noted to have prematurely grey hair (20) and patient 4 to have dark brown rather than black hair (21). This continues the unusual pigmentation defects found in the cblJ disorder, which, if present, may help distinguish it from other disorders of intracellular cobalamin metabolism.

FACS based FRET as a method to detect interaction – We have shown that specific interaction of LMBD1 and ABCD4 can be demonstrated using over-expression of each protein tagged to GFP and fRFP, respectively, and detected by a flow cytometer. Flow cytometry based FRET has been used previously to detect protein-protein interactions (e.g. (37,40,41)), primarily relying on cyan fluorescent protein (CFP) and yellow fluorescent protein (YFP) as conjugate pairs. Here, we show that a combination of GFP and fRFP can also be used, further opening this method to almost any flow cytometer currently in use. Although it is generally recommended to try both N-terminal and C-terminal fluorescent protein fusions, this may not be feasible for investigation of membrane proteins. We used exclusively C-terminal fusions, as only the C-terminus of all four proteins studied were predicted to extend into the cytosol (ABCD4: (4); LMBD1: (5); LAMP1: (42); ABCB9: (43)), thus enabling us to avoid signal loss from measuring FRET across a lipid membrane or from decreased EGFP emission intensity from low pH conditions (44), as is found inside late endosomes and lysosomes.

Potential cellular location of the LMBD1-ABCD4 complex – There are discrepancies within the literature concerning the cellular location of both LMBD1 and ABCD4. LMBD1 has been shown to localize to the lysosome (5), although a

later study using surface protein biotinylation found that ~3-4% of LMBD1 is located at the plasma membrane (15). We provide additional evidence of lysosomal localization via colocalization of LMBD1 with LAMP1 and LysoTracker using confocal microscopy. Our experiments cannot rule out that a small percentage of LMBD1 may also reside at the plasma membrane. Over-expressed ABCD4 alone has been reported to localize to the endoplasmic reticulum based on two papers from the same group (30,31). Also using over-expression, here no convincing colocalization with the ER was observed. Indeed, in all experiments wt ABCD4-fRFP was found with a punctate distribution in the perinucleus and across the cytoplasm. Classical routes for protein sorting to the lysosomal membrane consist of (i) the biosynthetic route, which involves secretion from the trans-Golgi network via late endosomes, with or without passing through early endosomes, and (ii) the endocytic route, which requires invagination from the plasma membrane with transition from early to late endosomes (45,46). However, no colocalization of ABCD4 with markers of the early, late, or recycling endosomes was found. Instead, the greatest overlap we found was between ABCD4-fRFP and LC3, a marker of autophagosomes. This autophagosomal localization might represent the degradation of ABCD4 molecules overexpressed in the absence of LMBD1, while the ER localization found by other groups might represent an earlier stage of ER retention by the protein quality control. It is thus tempting to speculate that ABCD4 molecules are unstable and, possibly, misfolded when they do not associate with LMBD1, suggesting a protective function of LMBD1 for ABCD4, in addition to mediating lysosomal targeting. Future experiments may clarify this potential secondary role for LMBD1.

We observed convincing co-localization between over-expressed wt ABCD4-fRFP and LMBD1-GFP in all cells examined. Based on further colocalization with LAMP1, this interaction appears to take place in the lysosomal membrane. This is consistent with the inability of cells with dysfunctional LMBD1 or ABCD4 to import cobalamin from the lysosome to the cytosol, and supports the role of this protein complex as being necessary for this export. This colocalization is consistent with previous studies (4), as is the requirement of LMBD1 to support ABCD4 lysosomal targeting (31).

Expression of ABCD4-fRFP alone resulted in increased AdoCbl and MeCbl cofactor synthesis in cblJ patient fibroblasts. Unexpectedly, cofactor synthesis was not further increased by co-transfection with LMBD1-GFP. While we cannot rule out that some ABCD4-fRFP makes its way to the lysosome, aided by the low levels of endogenous LMBD1 expected to be present in these cells, based on our colocalization results, co-expression with LMBD1-GFP would be expected to further increase lysosomal targeting. The lack of increased cofactor synthesis in the co-transfected cells suggests either that the small amount of correctly targeted ABCD4 is enough to mediate Cbl cofactor synthesis in these cells, or that a step downstream in the Cbl pathway is already saturated.

Mutational interference of protein-protein interaction – We constructed mutations within the Walker A and Walker B motifs of ABCD4. Single mutations affecting the Walker A motif (p.Gly426Ala and p.Lys427Leu, Suppl Figure S8) did not have a large effect on either protein function, as determined by the CCS assay, or interaction with LMBD1. In contrast the double mutation - (p.Gly426_Lys427delinsAlaLeu) and the Walker B mutation (p.Asp548Asn) - severely inhibited both function and interaction. These results strongly support the idea that ATPase activity of ABCD4 is required for interaction with LMBD1. Nucleotide-sensitive interaction has been documented for the association of ABCC8 or ABCC9 (also called SUR1 and SUR2) with Kir6.2, which together compose an ATP-sensitive potassium ion channel (47). In this complex, ATPase activity of the ABC-transporters is translated into ion channel opening of the associated Kir6.2 composed channel (48). Within the intracellular B12 metabolic pathway, interaction of the soluble mitochondrial proteins MMAA and MUT is dependent on GTP-binding of MMAA (49). In both cases, and perhaps for ABCD4 as well, nucleotide-binding and/or cleavage results in conformational changes to which its associated protein is sensitive.

Recapitulation of the patient mutations p.Asn141Lys and p.Arg432Gln gave similar but less severe results. FRET positive signal was decreased compared to wt ABCD4 for both mutant proteins, but not completely abolished, in line with decreased but still detectable cofactor synthesis. This decreased signal is unlikely to be due to protein misfolding, since the amount of ABCD-fRFP detected in the FACS assay and Western blot was

only slightly decreased for the mutant proteins compared to that of wild-type. The mutant proteins were also able to reach the lysosome, as indicated by colocalization with LMBD1. Therefore, the dysfunction caused by these mutations likely relates to a loss of function, e.g. p.Arg432Gln lies very close to the ATPase Walker A site, or, more likely, the decreased interaction with LMBD1. Consistent with the latter explanation, our homology model predicts Arg432 to face away from the nucleotide, on an α -helix that is accessible to the surface for protein binding. This mutation, then, may fall in line with the “interaction breaking” type mutations. Since protein-protein interactions are increasingly being recognized as crucial for proper intracellular cobalamin cofactor synthesis within the mitochondrial (49) and cytosolic B₁₂ pathways (9,50), it follows that the same would be true for the lysosome, and any mutational disruption of these interactions, in a manner similar to the other parts of the pathway (9,49), results in disease.

EXPERIMENTAL PROCEDURES

Cloning of expression vectors – DNA fragments encoding LMBD1 and ABCD4 in pTracer-CMV2, as described in (4), as well as LAMP1 (Addgene plasmid: 34831; (51)) and ABCB9 (OriGene) were amplified and cloned in frame with a C-terminal green fluorescent protein (GFP; pEGFP-N1, Clontech) or a far red fluorescent protein (fRFP; pmKate2-N, Evrogen) using the primers and restriction sites outlined in Suppl Table S1. A DNA fragment encoding ABCD3 (Origene) was amplified and cloned in frame with C-terminal GFP (pEGFP-N1) using the primers and restriction sites outlined in Suppl Table S1. GFP fused to fRFP was created by amplification of GFP from pEGFP-N1 and cloned into pmKate2-N using the primers and restriction sites outlined in Suppl Table S1. LMBD1-GFP fused to ABCD4-fRFP was created by cutting out LMBD1-GFP from pEGFP-N1 using HindIII and annealing it into ABCD4-fRFP pre-cut with HindIII. An in frame linker was then inserted between GFP and ABCD4 containing the protein sequence (GGGS)₃ using the overlapping DNA sequences

(forward)	5'-
GTACAAGTATGGCGGAGGTGGATCTGGCG	
GAGGTGGATCGGGCGGAGGTGGATCAAGC	
TTT-3'	5'-
and	(reverse)
GTACAAAGCTTGATCCACCTCCGCCCGATC	
CACCTCCGCCAGATCCACCTCCGCCATACT	
T-3'	

and cutting with the restriction enzymes BsrGI

and HindIII. Site-directed mutations were constructed with the QuikChange mutagenesis kit (Stratagene), with primers available upon request. EEA (in pEGFP-C1, (52)), Rab7 (in pEGFP-C1, (53)) and Rab11 (in pEGFP-C1, (53)) were purchased from Addgene. All constructs were confirmed by Sanger sequencing and prepared using the Plasmid Maxi kit (Qiagen) following manufacturer's instructions.

Cell culture and expression – Immortalized and primary patient fibroblasts, and immortalized control fibroblasts, were grown in Dulbecco's Modified Eagle's Medium (DMEM; Gibco) supplemented with 10 % foetal calf serum (FCS; Gibco) and antibiotics (PAA). HeLa cells were cultured in DMEM 4.5 g/l glucose supplemented with 10% FBS and 1% penicillin/streptomycin. All cells were cultured at 37°C with 5% CO₂. HeLa cells were transfected by lipofection with lipofectamine 2000 (Thermo Fisher Scientific) according to manufacturer's instructions. For fibroblasts, electroporation was performed as described previously (54), using 15-25 µg DNA for single transfections and, in co-transfections, 10-12.5 µg DNA per donor construct and 10-12.5 µg DNA per acceptor construct.

Flow cytometry-based FRET – Flow cytometry measurements were performed 30-40 h post transfection using a FACSAriaIII (BD Bioscience). Transfected cells were excited at 488 nm and 561 nm; photomultiplier tube (PMT), voltages and compensation for GFP and fRFP were adjusted using the BD FACSDiva 7.0 software. GFP was excited with the 488 nm laser and measured with a 540/30 filter, any occurring FRET-signal was measured with a 695/40 filter. fRFP was excited with the 561 nm laser and measured with a 610/20 filter. For each sample 30'000 events were collected. Data were analyzed and visualized using FlowJo (version 10) software. Experiments were performed in immortalized wild-type, cblJ02 and cblF fibroblasts. Since we found no difference in FRET-positive signal based on cell lineage, the data for experiments in each cell type were pooled.

Confocal and epifluorescence microscopy – To analyse subcellular localization, immortalized control fibroblasts or HeLa cells co-transfected with selected constructs were grown on glass slides (CultureSlides; BD Falcon), fixed after 30-40 h post transfection with 4% paraformaldehyde for 20 minutes, washed three times in PBS (10 mM Na₂HPO₄, 2 mM KH₂PO₄, 137 mM NaCl, 2.7 mM

KCl) and mounted onto a coverslip using SlowFade Gold antifade mountant (S36939; Molecular Probes) containing 4'-6-diamidion-2-phenylindole (DAPI) for nuclear staining. For antibody staining of anti-HSP47, cells were fixed in ice-cold methanol for 5 min, washed three times in PBS and incubated in blocking buffer (10% FCS, 0.1% Tween 20 in PBS) for 1 h at room temperature. For all other antibodies, the cells were fixed with 4% paraformaldehyde washed 3-times in PBS and permeabilized with 0.1% Triton X-100 in PBS for 15 min followed by 3-times washing with PBS containing 100 mM glycine and incubation in blocking buffer (10% FCS, 0.1% Tween 20 in PBS) for 1 h at room temperature. Cells were then incubated with primary antibody (mouse anti-HSP47, Enzo Life Sciences, diluted 1:1000; mouse anti-LAMP1, Developmental Studies Hybridoma Bank clone H4A3, diluted to 0.75 µg/ml) in blocking buffer for 1.5 h at room temperature, followed by washing three times in PBS and incubation with secondary antibody (goat anti-mouse Alexa Fluor 488 or goat anti-mouse Alexa Fluor 405, Life Technologies) diluted 1:500 in blocking buffer for 30 min at room temperature. After washing three times in PBS, the coverslips were mounted onto glass slides using ProLong Diamond antifade mountant with or without DAPI (Life Technologies). Images were taken on a confocal (Leica SP5) or epifluorescent microscope, and analyzed by the JACoP v2.0 plug-in for ImageJ (55).

Cobalamin coenzyme synthesis (CCS) assay – Uptake of [⁵⁷Co]cyanocobalamin and synthesis of the cobalamin coenzyme forms, AdoCbl and MeCbl, from [⁵⁷Co]cyanocobalamin in intact cells were performed as described (56). Unless otherwise specified, immortalized cblF and cblJ02 fibroblasts were used for all CCS assays (for mutation description see Table 1).

Homology modeling and ligand docking – A 3D model of the ATPase domain of human ABCD4 (residues 386 to 605) was built using Modeller9v8 (57) and the crystal structure of the multiple sugar binding transport ATP-binding protein from *Pyrococcus horikoshii* (PDB ID # 2D62). To optimize the alignment between these two sequences, a multiple alignment including another crystallized ABC transporter, the peptidase-containing ABC transporter PCAT1 from *Ruminiclostridium thermocellum* (ID # 4RY2), homologous to human ABCD4 beyond the ATPase

domain (22% identity over 398 amino acids) was made using Clustal Omega and manually refined to superimpose secondary structures of the two crystallized proteins. The ATPase domains of human ABCD4 and of the *P. horikoshii* multiple sugar transporter show 30% identity and 35% similarity. One-hundred 3D models were generated and evaluated by their DOPE (Discrete Optimized Protein Energy) and GA341 scores calculated by Modeller. Validation steps were applied to the five best models (corresponding to the lowest DOPE scores) using PROCHECK (58), WHAT_CHECK (59), ERRAT (60) and VERIFY_3D (61). The final model was the best one according to a compromise between the four programs.

This 3D model was then refined by several cycles of minimization and equilibrated by molecular dynamics simulations (1-ns runs) using the CHARMM force field. Bonds involving hydrogen atoms were constrained using the SHAKE

algorithm (62). At the end of each optimization, the final structure was controlled using PROCHECK and VERIFY_3D. The Ramachandran plot of the final 3D model showed 86% (188/220) favoured, 12% (27/220) allowed and 2% (2 Glu and 3 Gly) disallowed residues. A solvent box with a periodic boundary of 9 Å was added to the ABCD4 model. Solvation was completed with 0.145 M KCl using the DS 4.5 solvation protocol. The model was then minimized using Adopted Basis NR algorithm with an average gradient ≤ 0.001 kcal/mol.Å. Non-specific water molecules were removed and ADP molecules were docked to the 3D model using C-Docker (63) from Discovery Studio 4.5 (Accelrys, Dassault Systems Biovia, Meudon, France), with default parameters and a sphere radius of 10 Å. The poses showing the lowest -cDock interaction energy as scoring function were retained and clustered according to their binding mode.

Acknowledgements: This work was supported by the Swiss National Science Foundation (SNSF 31003A_156907, to M.R.B.) and the Rare Disease Initiative Zurich (radiz), a clinical research priority program for rare diseases of the University of Zurich, Switzerland. Imaging was performed with support of the Center for Microscopy and Image Analysis, University of Zurich.

Conflict of interest: The authors declare that they have no conflicts of interest with the contents of this article.

Author contributions: DC, BF, DSF and MRB conceived the idea of the project. VF designed the research together with PB, CS, BG, DSF and MRB. VF performed most of the experiments. Experimental work was also carried out by PB, CS, DC, and BB. CDL provided clinical data. NP and BG generated the homology model. SL and TS performed the experiments to determine the cblJ defect in the patient. VF and DSF wrote the paper with contributions from the other authors. All authors analyzed the results and approved the final version of the manuscript.

REFERENCES

1. Banerjee, R., Gherasim, C., and Padovani, D. (2009) The tinker, tailor, soldier in intracellular B12 trafficking. *Curr Opin Chem Biol* **13**, 484-491
2. Froese, D. S., and Gravel, R. A. (2010) Genetic disorders of vitamin B metabolism: eight complementation groups--eight genes. *Expert Rev Mol Med* **12**, e37
3. Quadros, E. V., and Sequeira, J. M. (2013) Cellular uptake of cobalamin: transcobalamin and the TCblR/CD320 receptor. *Biochimie* **95**, 1008-1018
4. Coelho, D., Kim, J. C., Miousse, I. R., Fung, S., du Moulin, M., Buers, I., Suormala, T., Burda, P., Frapolli, M., Stucki, M., Nurnberg, P., Thiele, H., Robenek, H., Hohne, W., Longo, N., Pasquali, M., Mengel, E., Watkins, D., Shoubbridge, E. A., Majewski, J., Rosenblatt, D. S., Fowler, B., Rutsch, F., and Baumgartner, M. R. (2012) Mutations in ABCD4 cause a new inborn error of vitamin B12 metabolism. *Nat Genet* **44**, 1152-1155
5. Rutsch, F., Gailus, S., Miousse, I. R., Suormala, T., Sagne, C., Toliat, M. R., Nurnberg, G., Wittkamp, T., Buers, I., Sharifi, A., Stucki, M., Becker, C., Baumgartner, M., Robenek, H.,

- Marquardt, T., Hohne, W., Gasnier, B., Rosenblatt, D. S., Fowler, B., and Nurnberg, P. (2009) Identification of a putative lysosomal cobalamin exporter altered in the cblF defect of vitamin B12 metabolism. *Nat Genet* **41**, 234-239
6. Hannibal, L., Kim, J., Brasch, N. E., Wang, S., Rosenblatt, D. S., Banerjee, R., and Jacobsen, D. W. (2009) Processing of alkylcobalamins in mammalian cells: A role for the MMACHC (cblC) gene product. *Mol Genet Metab* **97**, 260-266
7. Kim, J., Gherasim, C., and Banerjee, R. (2008) Decyanation of vitamin B12 by a trafficking chaperone. *Proc Natl Acad Sci U S A* **105**, 14551-14554
8. Suormala, T., Baumgartner, M. R., Coelho, D., Zavadakova, P., Kozich, V., Koch, H. G., Berghauer, M., Wraith, J. E., Burlina, A., Sewell, A., Herwig, J., and Fowler, B. (2004) The cblD defect causes either isolated or combined deficiency of methylcobalamin and adenosylcobalamin synthesis. *J Biol Chem* **279**, 42742-42749
9. Froese, D. S., Kopec, J., Fitzpatrick, F., Schuller, M., McCorvie, T. J., Chalk, R., Plessl, T., Fettelschoss, V., Fowler, B., Baumgartner, M. R., and Yue, W. W. (2015) Structural Insights into the MMACHC-MMADHC Protein Complex Involved in Vitamin B12 Trafficking. *J Biol Chem* **290**, 29167-29177
10. Padovani, D., Labunska, T., Palfey, B. A., Ballou, D. P., and Banerjee, R. (2008) Adenosyltransferase tailors and delivers coenzyme B-12. *Nature Chemical Biology* **4**, 194-196
11. Padovani, D., and Banerjee, R. (2009) A G-protein editor gates coenzyme B12 loading and is corrupted in methylmalonic aciduria. *Proc Natl Acad Sci U S A* **106**, 21567-21572
12. Rosenblatt, D. S., Hosack, A., Matiaszuk, N. V., Cooper, B. A., and Laframboise, R. (1985) Defect in vitamin B12 release from lysosomes: newly described inborn error of vitamin B12 metabolism. *Science* **228**, 1319-1321
13. Watkins, D., and Rosenblatt, D. S. (1986) Failure of lysosomal release of vitamin B12: a new complementation group causing methylmalonic aciduria (cblF). *Am J Hum Genet* **39**, 404-408
14. Dufour, E., Marden, M. C., and Haertle, T. (1990) Beta-lactoglobulin binds retinol and protoporphyrin IX at two different binding sites. *FEBS Lett* **277**, 223-226
15. Tseng, L. T., Lin, C. L., Tzen, K. Y., Chang, S. C., and Chang, M. F. (2013) LMBD1 protein serves as a specific adaptor for insulin receptor internalization. *J Biol Chem* **288**, 32424-32432
16. Gailus, S., Suormala, T., Malerczyk-Aktas, A. G., Toliat, M. R., Wittkamp, T., Stucki, M., Nurnberg, P., Fowler, B., Hennermann, J. B., and Rutsch, F. (2010) A novel mutation in LMBRD1 causes the cblF defect of vitamin B(12) metabolism in a Turkish patient. *J Inherit Metab Dis* **33**, 17-24
17. Alfadhel, M., Lillquist, Y. P., Davis, C., Junker, A. K., and Stockler-Ipsiroglu, S. (2011) Eighteen-year follow-up of a patient with cobalamin F disease (cblF): report and review. *Am J Med Genet A* **155A**, 2571-2577
18. Oladipo, O., Rosenblatt, D. S., Watkins, D., Miousse, I. R., Sprietsma, L., Dietzen, D. J., and Shinawi, M. (2011) Cobalamin F disease detected by newborn screening and follow-up on a 14-year-old patient. *Pediatrics* **128**, e1636-1640
19. Armour, C. M., Brebner, A., Watkins, D., Geraghty, M. T., Chan, A., and Rosenblatt, D. S. (2013) A patient with an inborn error of vitamin B12 metabolism (cblF) detected by newborn screening. *Pediatrics* **132**, e257-261
20. Kim, J. C., Lee, N. C., Hwu, P. W., Chien, Y. H., Fahiminiya, S., Majewski, J., Watkins, D., and Rosenblatt, D. S. (2012) Late onset of symptoms in an atypical patient with the cblJ inborn error of vitamin B12 metabolism: diagnosis and novel mutation revealed by exome sequencing. *Mol Genet Metab* **107**, 664-668
21. Takeichi, T., Hsu, C. K., Yang, H. S., Chen, H. Y., Wong, T. W., Tsai, W. L., Chao, S. C., Lee, J. Y., Akiyama, M., Simpson, M. A., and McGrath, J. A. (2015) Progressive hyperpigmentation in a Taiwanese child due to an inborn error of vitamin B12 metabolism (cblJ). *Br J Dermatol* **172**, 1111-1115

22. Pahadiya, H. R., Lakhotia, M., Choudhary, S., Prajapati, G. R., and Pradhan, S. (2016) Reversible ecchymosis and hyperpigmented lesions: A rare presentation of dietary Vitamin B12 deficiency. *J Family Med Prim Care* **5**, 485-487
23. Santra, G., Paul, R., Ghosh, S. K., Chakraborty, D., Das, S., Pradhan, S., and Das, A. (2014) Generalised hyperpigmentation in vitamin B12 deficiency. *J Assoc Physicians India* **62**, 714-716
24. Hatzimichael, E., and Briasoulis, E. (2016) Megaloblastic anemia presenting with skin hyperpigmentation. *Int J Hematol* **103**, 479-480
25. Kamijo, K., Taketani, S., Yokota, S., Osumi, T., and Hashimoto, T. (1990) The 70-kDa peroxisomal membrane protein is a member of the Mdr (P-glycoprotein)-related ATP-binding protein superfamily. *J Biol Chem* **265**, 4534-4540
26. Lombard-Platet, G., Savary, S., Sarde, C. O., Mandel, J. L., and Chimini, G. (1996) A close relative of the adrenoleukodystrophy (ALD) gene codes for a peroxisomal protein with a specific expression pattern. *Proc Natl Acad Sci U S A* **93**, 1265-1269
27. Contreras, M., Mosser, J., Mandel, J. L., Aubourg, P., and Singh, I. (1994) The protein coded by the X-adrenoleukodystrophy gene is a peroxisomal integral membrane protein. *FEBS Lett* **344**, 211-215
28. Mosser, J., Lutz, Y., Stoeckel, M. E., Sarde, C. O., Kretz, C., Douar, A. M., Lopez, J., Aubourg, P., and Mandel, J. L. (1994) The gene responsible for adrenoleukodystrophy encodes a peroxisomal membrane protein. *Hum Mol Genet* **3**, 265-271
29. Lee, A., Asahina, K., Okamoto, T., Kawaguchi, K., Kostsin, D. G., Kashiwayama, Y., Takanashi, K., Yazaki, K., Imanaka, T., and Morita, M. (2014) Role of NH2-terminal hydrophobic motif in the subcellular localization of ATP-binding cassette protein subfamily D: common features in eukaryotic organisms. *Biochem Biophys Res Commun* **453**, 612-618
30. Kashiwayama, Y., Seki, M., Yasui, A., Murasaki, Y., Morita, M., Yamashita, Y., Sakaguchi, M., Tanaka, Y., and Imanaka, T. (2009) 70-kDa peroxisomal membrane protein related protein (P70R/ABCD4) localizes to endoplasmic reticulum not peroxisomes, and NH2-terminal hydrophobic property determines the subcellular localization of ABC subfamily D proteins. *Exp Cell Res* **315**, 190-205
31. Kawaguchi, K., Okamoto, T., Morita, M., and Imanaka, T. (2016) Translocation of the ABC transporter ABCD4 from the endoplasmic reticulum to lysosomes requires the escort protein LMBD1. *Sci Rep* **6**, 30183
32. Chapel, A., Kieffer-Jaquinod, S., Sagne, C., Verdon, Q., Ivaldi, C., Mellal, M., Thirion, J., Jadot, M., Bruley, C., Garin, J., Gasnier, B., and Journet, A. (2013) An extended proteome map of the lysosomal membrane reveals novel potential transporters. *Mol Cell Proteomics* **12**, 1572-1588
33. Deme, J. C., Hancock, M. A., Xia, X., Shintre, C. A., Plesa, M., Kim, J. C., Carpenter, E. P., Rosenblatt, D. S., and Coulton, J. W. (2014) Purification and interaction analyses of two human lysosomal vitamin B12 transporters: LMBD1 and ABCD4. *Mol Membr Biol* **31**, 250-261
34. Chan, F. K., Siegel, R. M., Zacharias, D., Swofford, R., Holmes, K. L., Tsien, R. Y., and Lenardo, M. J. (2001) Fluorescence resonance energy transfer analysis of cell surface receptor interactions and signaling using spectral variants of the green fluorescent protein. *Cytometry* **44**, 361-368
35. He, L., Olson, D. P., Wu, X., Karpova, T. S., McNally, J. G., and Lipsky, P. E. (2003) A flow cytometric method to detect protein-protein interaction in living cells by directly visualizing donor fluorophore quenching during CFP-->YFP fluorescence resonance energy transfer (FRET). *Cytometry A* **55**, 71-85
36. You, X., Nguyen, A. W., Jabaiah, A., Sheff, M. A., Thorn, K. S., and Daugherty, P. S. (2006) Intracellular protein interaction mapping with FRET hybrids. *Proc Natl Acad Sci U S A* **103**, 18458-18463
37. Banning, C., Votteler, J., Hoffmann, D., Koppensteiner, H., Warmer, M., Reimer, R., Kirchhoff, F., Schubert, U., Hauber, J., and Schindler, M. (2010) A flow cytometry-based FRET assay to identify and analyse protein-protein interactions in living cells. *PLoS One* **5**, e9344
38. Hagen, N., Bayer, K., Rosch, K., and Schindler, M. (2014) The intraviral protein interaction network of hepatitis C virus. *Mol Cell Proteomics* **13**, 1676-1689

39. (2016) SSIEM 2016 Annual Symposium - Abstracts : Rome, Italy, September 2016. *J Inherit Metab Dis* **39 Suppl 1**, 35-284
40. Wu, X., Currall, B., Yamashita, T., Parker, L. L., Hallworth, R., and Zuo, J. (2007) Prestin-prestin and prestin-GLUT5 interactions in HEK293T cells. *Dev Neurobiol* **67**, 483-497
41. Thyrock, A., Stehling, M., Waschbusch, D., and Barnekow, A. (2010) Characterizing the interaction between the Rab6 GTPase and Mint3 via flow cytometry based FRET analysis. *Biochem Biophys Res Commun* **396**, 679-683
42. Cook, N. R., Row, P. E., and Davidson, H. W. (2004) Lysosome associated membrane protein 1 (Lamp1) traffics directly from the TGN to early endosomes. *Traffic* **5**, 685-699
43. Zhao, C., Tampe, R., and Abele, R. (2006) TAP and TAP-like--brothers in arms? *Naunyn Schmiedebergs Arch Pharmacol* **372**, 444-450
44. Haupts, U., Maiti, S., Schwille, P., and Webb, W. W. (1998) Dynamics of fluorescence fluctuations in green fluorescent protein observed by fluorescence correlation spectroscopy. *Proc Natl Acad Sci U S A* **95**, 13573-13578
45. Bonifacino, J. S., and Traub, L. M. (2003) Signals for sorting of transmembrane proteins to endosomes and lysosomes. *Annu Rev Biochem* **72**, 395-447
46. Jeyakumar, M., Dwek, R. A., Butters, T. D., and Platt, F. M. (2005) Storage solutions: treating lysosomal disorders of the brain. *Nat Rev Neurosci* **6**, 713-725
47. Locher, K. P. (2016) Mechanistic diversity in ATP-binding cassette (ABC) transporters. *Nat Struct Mol Biol* **23**, 487-493
48. Aittoniemi, J., Fotinou, C., Craig, T. J., de Wet, H., Proks, P., and Ashcroft, F. M. (2009) Review. SUR1: a unique ATP-binding cassette protein that functions as an ion channel regulator. *Philos Trans R Soc Lond B Biol Sci* **364**, 257-267
49. Froese, D. S., Kochan, G., Muniz, J. R., Wu, X., Gileadi, C., Ugochukwu, E., Krysztofinska, E., Gravel, R. A., Oppermann, U., and Yue, W. W. (2010) Structures of the human GTPase MMAA and vitamin B12-dependent methylmalonyl-CoA mutase and insight into their complex formation. *J Biol Chem* **285**, 38204-38213
50. Bassila, C., Ghemrawi, R., Flayac, J., Froese, D. S., Baumgartner, M. R., Gueant, J. L., and Coelho, D. (2017) Methionine synthase and methionine synthase reductase interact with MMACHC and with MMADHC. *Biochim Biophys Acta* **1863**, 103-112
51. Falcon-Perez, J. M., Nazarian, R., Sabatti, C., and Dell'Angelica, E. C. (2005) Distribution and dynamics of Lamp1-containing endocytic organelles in fibroblasts deficient in BLOC-3. *J Cell Sci* **118**, 5243-5255
52. Lawe, D. C., Patki, V., Heller-Harrison, R., Lambright, D., and Corvera, S. (2000) The FYVE domain of early endosome antigen 1 is required for both phosphatidylinositol 3-phosphate and Rab5 binding. Critical role of this dual interaction for endosomal localization. *J Biol Chem* **275**, 3699-3705
53. Choudhury, A., Dominguez, M., Puri, V., Sharma, D. K., Narita, K., Wheatley, C. L., Marks, D. L., and Pagano, R. E. (2002) Rab proteins mediate Golgi transport of caveola-internalized glycosphingolipids and correct lipid trafficking in Niemann-Pick C cells. *J Clin Invest* **109**, 1541-1550
54. Burda, P., Suormala, T., Heuberger, D., Schafer, A., Fowler, B., Froese, D. S., and Baumgartner, M. R. (2017) Functional characterization of missense mutations in severe methylenetetrahydrofolate reductase deficiency using a human expression system. *J Inherit Metab Dis* **40**, 297-306
55. Bolte, S., and Cordelieres, F. P. (2006) A guided tour into subcellular colocalization analysis in light microscopy. *J Microsc* **224**, 213-232
56. Jusufi, J., Suormala, T., Burda, P., Fowler, B., Froese, D. S., and Baumgartner, M. R. (2014) Characterization of functional domains of the cblD (MMADHC) gene product. *J Inherit Metab Dis* **37**, 841-849
57. Sali, A., Potterton, L., Yuan, F., van Vlijmen, H., and Karplus, M. (1995) Evaluation of comparative protein modeling by MODELLER. *Proteins* **23**, 318-326

58. Laskowski, R. A., MacArthur, M. W., Moss, D. S., and Thornton, J. M. (1993) PROCHECK - a program to check the stereochemical quality of protein structures. *J App Cryst* **26**, 283-291
59. Hooft, R. W., Vriend, G., Sander, C., and Abola, E. E. (1996) Errors in protein structures. *Nature* **381**, 272
60. Colovos, C., and Yeates, T. O. (1993) Verification of protein structures: patterns of nonbonded atomic interactions. *Protein Sci* **2**, 1511-1519
61. Bowie, J. U., Luthy, R., and Eisenberg, D. (1991) A method to identify protein sequences that fold into a known three-dimensional structure. *Science* **253**, 164-170
62. Ciccotti, G., and Ryckaert, J. P. (1986) Molecular dynamics simulation of rigid molecules. *Comp Phys Reports* **4**, 346-392
63. Wu, G., Robertson, D. H., Brooks, C. L., 3rd, and Vieth, M. (2003) Detailed analysis of grid-based molecular docking: A case study of CDOCKER-A CHARMM-based MD docking algorithm. *J Comput Chem* **24**, 1549-1562

Table 1. Description of patients and cell lines used.

Cell Line	Patient #	Defect	Mutation 1	Mutation 2	Reference
WG4066	cbIJ01	cbIJ	c.955A>G (p.Tyr319Cys)	c.1747_1748insCT (p.Glu583Leufs*9)	(4)
cbIJ02	cbIJ02	cbIJ	c.542+1G>T (p.Asp143_Ser181del)	c.1456G>T (p.Gly443-Ser485del)	(5)
	cbIJ03	cbIJ	c.423C>G (p.Asn141Lys)	c.423C>G (p.Asn141Lys)	(10)
	cbIJ04	cbIJ	c.423C>G (p.Asn141Lys)	c.423C>G (p.Asn141Lys)	(11)
cbIJ05	cbIJ05	cbIJ	c.1295G>A (p.Arg432Gln)	c.1667_1668delAG (p.Glu556Glyfs*27)	This paper
cbIF		cbIF	c.1405delG (p.Asp469fs*38)	c.1405delG (p.Asp469fs*38)	(16)

Downloaded from <http://www.jbc.org/> by guest on July 16, 2017

Table 2. Normalization of clinical parameters following intense vitamin B₁₂ treatment.

Parameter	First visit at the age of 10y	4 months later
Total homocysteine (μmol/l)	57	8.4
Methylmalonic acid (mmol/mol creat)	64	2
Vitamin B12 (ng/l)	560	>2000
MCV of RBC (fl)	98	87
Methionine (μmol/l)	17 (N)	30 (N)
Albuminuria (mg/g creat)	94	17

FIGURE LEGENDS

FIGURE 1. Cobalamin cofactor synthesis rescue in cblF and cblJ patient fibroblasts. **A.** Transfection of *LMBRD1* (cblF) and *ABCD4* (cblJ) wild type (wt) alleles in immortalized fibroblasts of the two original patients with cblJ defect (cblJ01 and cblJ02), cblJ05 and a patient with the cblF defect. Transfections with empty vector (vector only) were used as negative controls. Mean plus standard deviation is shown. **B.** cblF patient fibroblasts were transfected with DNA coding for fluorescent protein only (GFP), untagged LMBD1 in pTracer-CMV2 (LMBD1) or fluorescently tagged-LMBD1 (LMBD1-GFP). cblJ patient fibroblasts were transfected with DNA coding for fluorescent protein only (fRFP), untagged ABCD4 in pTracer-CMV2 (ABCD4) or fluorescently tagged-ABCD4 (ABCD4-fRFP) +/- LMBD1-GFP. Immortalized control fibroblasts without transfection ($n = 23$,) are shown for comparison. Bars represent the mean and error bars standard deviation from at least 3 separate experiments.

FIGURE 2. Colocalization of ABCD4-fRFP and LMBD1-GFP with endogenous LAMP1. **A.** Confocal microscopy images of immortalized control fibroblasts co-transfected with LMBD1-GFP and ABCD4-fRFP and stained with LAMP1 antibody to localize lysosomes. **B.** LMBD1-GFP over-expression compared with LAMP1 staining. Regions in which both proteins co-localize appear yellow in the merged image. **C.** ABCD4-fRFP over-expression compared with LAMP1 staining. The absence of yellow in the merged image indicates lack of colocalization. For A-C, the white scale bar is 10 μ m. Arrowheads depict examples of overlap between all three markers.

FIGURE 3. Analysis of protein interactions in immortalized fibroblasts using flow cytometry-based FRET. **A.** Histogram view of GFP intensity (%GFP) and fRFP intensity (%fRFP) for each (co-)transfection. Cells were considered GFP+ or fRFP+ if intensity was above 10^2 in each respective channel. From cells that were GFP+ and fRFP+, the mean intensity (MI) of signal in the FRET channel was calculated. **B.** FRET intensity plotted against GFP intensity, where FRET+ cells are defined by a stick-shaped gate encompassing signal from conjugated LMBD1-ABCD4 above the intensity threshold of 10^2 for both GFP and FRET (left panel). Pictures depict a representative experiment, number in purple represents average percentage of all live cells that are FRET+ for each condition ($n \geq 3$). **C.** Bar graph of the percent FRET+ positive cells from those cells that were GFP+ and fRFP+ for each condition. Data represents at least 3 separate experiments. Error bar represents standard deviation. **D.** Table summarizing the data presented in panels B and C.

FIGURE 4. Missense mutations from patients and in the ATPase domain of ABCD4 can disrupt interaction with LMBD1. **A.** Left: FRET intensity plotted against GFP intensity, where FRET+ cells are defined as in Figure 3B. Number in purple represents percentage of all live cells that are FRET+ for each condition. Right: Bar graph of the percent FRET+ positive cells from those cells that were GFP+ and fRFP+ for each condition. For each mutation % FRET+ cells are given as percent wild-type ABCD4. Data represents at least 3 separate experiments. Error bar represents standard deviation. **B.** Merged confocal images of fibroblasts co-transfected with combinations of mutant ABCD4-fRFP and wild-type LMBD1-GFP. Regions in which both proteins co-localize appear yellow. White square indicates zoomed in region below. Scale bar is 10 μ m. Numbers indicate Pearson correlation coefficient. **C.** Rescue of AdoCbl and MeCbl synthesis in immortalized fibroblasts of an ABCD4-deficient (cblJ02) patient following transfection with mutant ABCD4-fRFP proteins. Error bar represents standard deviation. Data represents a single experiment performed in triplicate.

FIGURE 5. Homology modeling of the ATPase domain of ABCD4. **A.** Schematic of ABCD4 protein sequence (top) and topology (bottom) with location of mutations used in the study indicated. Sequence and topology as described in (4). The ATP domain highlighted in grey is the region used to generate the homology model (see also Suppl Figure S9). **B.** Two views of the ATPase domain model showing secondary structures (grey ribbon), an ADP molecule docked to the nucleotide-binding site and the side chain of the residue (R432) affected by the missense CblJ patient fifth mutation.

Figure 1.

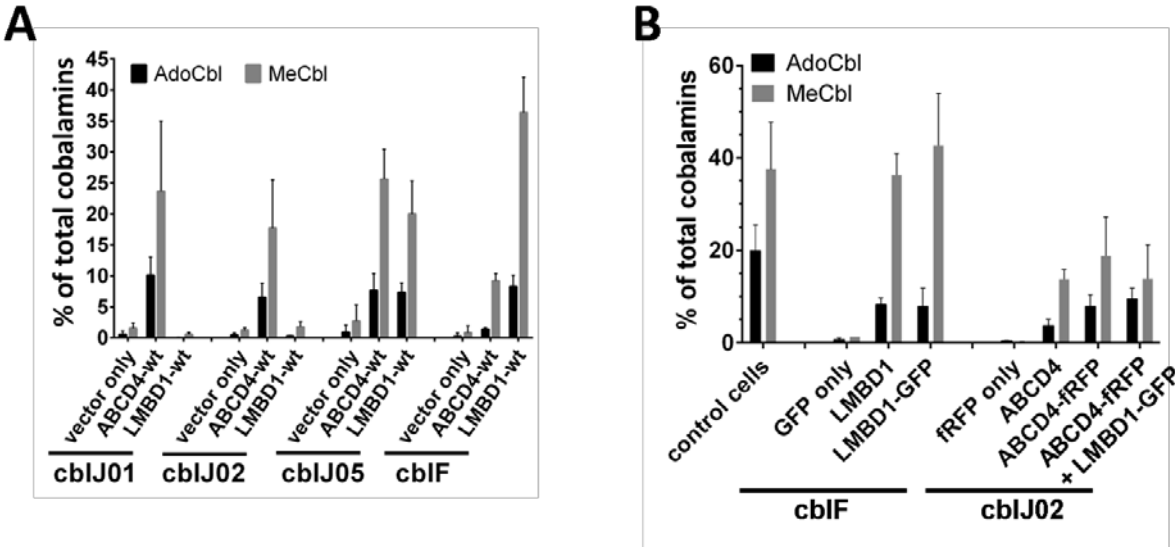


Figure 2.

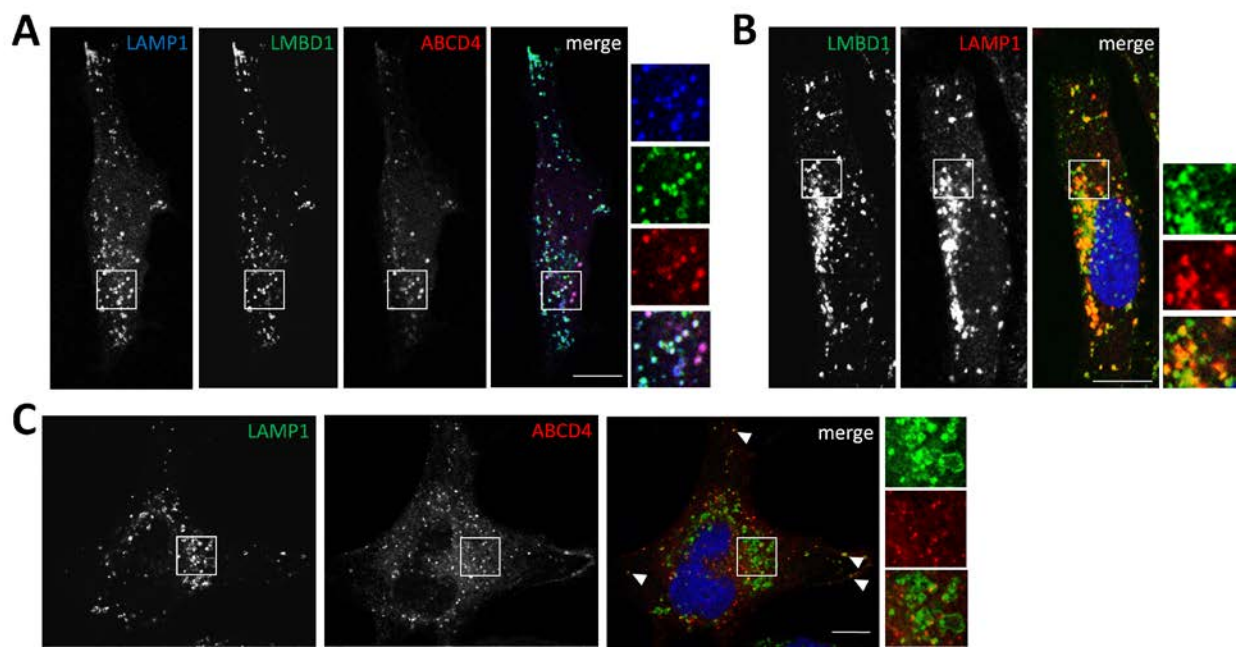


Figure 3.

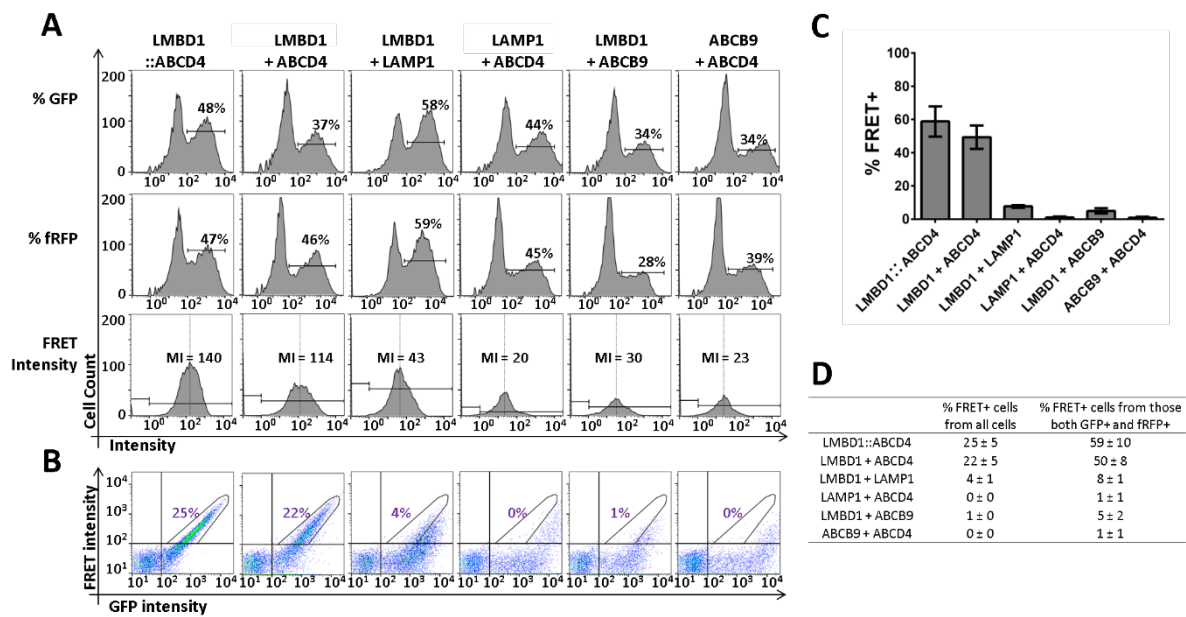


Figure 4.

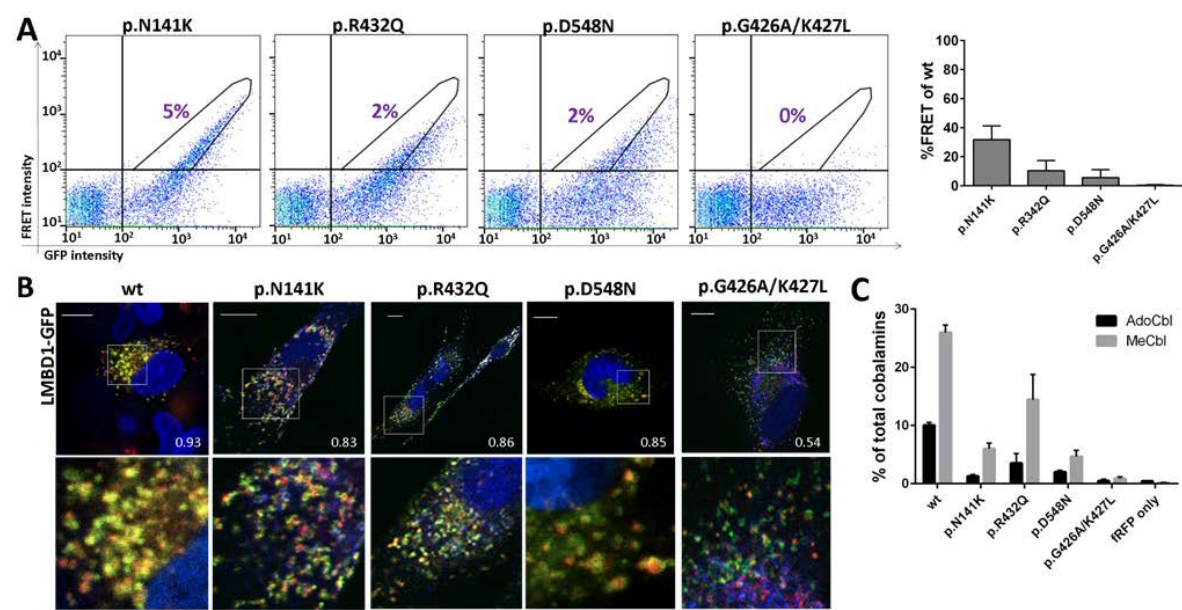
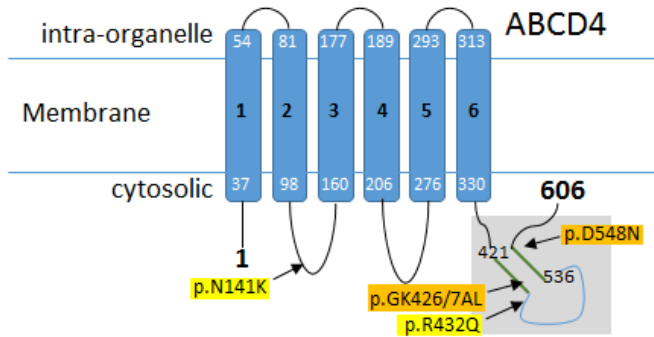


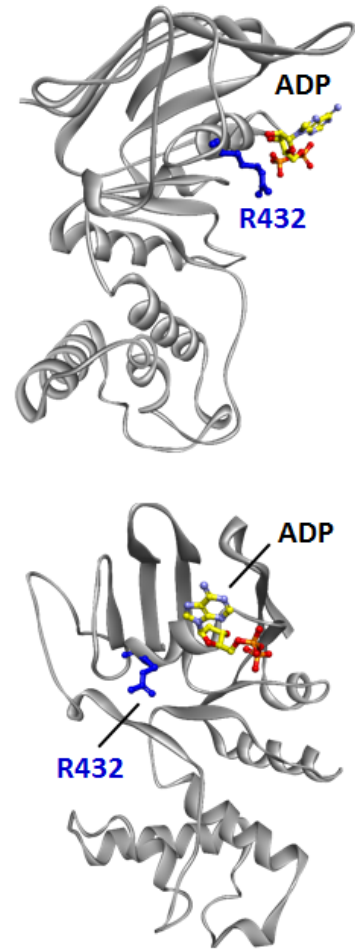
Figure 5.

A MAVAGPAPGAGARPRLDLQFLQRFLQILKVLFPWS¹SQNALMFLTL
LCLTLLEQFVIYQVGLIPSQYYGVLGNDLEGFK²TLTFLAVMLIVLNSTL
KSFQDFTCNLLYVSWRKDLTEHLHRLYFRGRAYTINVLRDDID³NPDQ
RISQDVERFCRQLSS³MASKLIISPFTLVYYTYQCFQSTGWLGVPV⁴SIFG
YFILGTVVNKTLMGPIVMKLVHQEKLEGDFRFKHMQRVNAEPAAFY
RAGHVEHMRTDRRLQRLQLTQRELMSELWLYIGIN⁵TFDYLGSLISY
VVIAPIFSGVYGDLSPTLSTLVSK⁶NAFVCIYLISCFTQLIDLSTTLSDVA
GYTHRIGQLRETLDDMSLSQDCEILGESKWGLDTPPGWPAAEPADT
AFLERVSISAPSSDKPLIKDLSLKISEGQSLIT⁶GNTGTGK⁶SLLRVLGGL
WTSTRGSVQMLTDFGPHGVLFPLPQKPFETDGTLRQVIYPLKEVYPDS
GSADDERILRFELEAGLSNLVARTEGLDQQVDWNWYDVLSPGEMQR
LSFARLFYLPKYAVLD⁶EATSALTEEVESELYRIGQQLGMTFISVGHRQ
SLEKFHSLVLKLCGGGRWELMRIKVEC

- Transmembrane helices
- Walker A and B motifs
- ATP Domain
- Patient mutations
- ATPase mutations



B



Clinical or ATPase domain mutations in ABCD4 disrupt the interaction between the vitamin B12-trafficking proteins ABCD4 and LMBD1

Victoria Fettelschoss, Patricie Burda, Corinne Sagné, David Coelho, Corinne De Laet, Seraina Lutz, Terttu Suormala, Brian Fowler, Nicolas Pietrancosta, Bruno Gasnier, Beat Bornhauser, D. Sean Froese and Matthias R. Baumgartner

J. Biol. Chem. published online June 1, 2017

Access the most updated version of this article at doi: [10.1074/jbc.M117.784819](https://doi.org/10.1074/jbc.M117.784819)

Alerts:

- [When this article is cited](#)
- [When a correction for this article is posted](#)

[Click here](#) to choose from all of JBC's e-mail alerts

Supplemental material:

<http://www.jbc.org/content/suppl/2017/06/01/M117.784819.DC1>

This article cites 0 references, 0 of which can be accessed free at

<http://www.jbc.org/content/early/2017/06/01/jbc.M117.784819.full.html#ref-list-1>